Journal of *Marine Science and Engineering*

MDPI

Article

A Study on the Response of Coral Sand Foundations with Different Particle Gradations Reinforced Using a Vibroflotation Method

Yiwen Xin [1,2], Xuanming Ding [1,2,*], Jinqiao Zhao [1,2], Hong Wang [1,2] and Chunyong Jiang [3]

[1] College of Civil Engineering, Chongqing University, Chongqing 400045, China; xywcqu@163.com (Y.X.); zjqiao_cqu@163.com (J.Z.); wh@stu.cqu.edu.cn (H.W.)
[2] Key Laboratory of New Technology for Construction of Cities in Mountain Area, Chongqing University, Chongqing 400045, China
[3] Chongqing City Construction Investment (Group), Chongqing 400015, China; chiangchunyung@163.com
* Correspondence: dxmhhu@163.com

Abstract: Vibroflotation has proven to be an effective method for treating loose and unevenly graded coral sand foundations formed through hydraulic filling. In this study, a series of model tests were conducted to investigate the effects of particle gradations on the response of coral sand foundation reinforced by vibroflotation. The main focus was on analyzing the changes in excess pore water pressure (EPWP) and horizontal earth pressure. Cone penetration tests (CPTs) were then used to evaluate the effectiveness of vibroflotation. The results indicate that the maximum settlement occurs after the first vibroflotation, with surface settlement significantly increasing as the distance to the vibro-point decreases. The reinforcement range expands radially, and the foundation can achieve a medium or dense state after vibroflotation. During the penetration stage, the EPWP rapidly peaks and increases with depth. Shallow foundations exhibit a higher excess pore pressure ratio compared to deep foundations. Foundations with lower coarse particle content show higher EPWPs compared to those with higher coarse particle content. Lower vibration frequency results in diminished reinforcement effects in foundations with high coarse particle content and increases the difficulty of penetration. Additionally, the residual soil pressure in foundations with high coarse particle content significantly rises after three vibroflotation reinforcements. The increase in strength after reinforcement is more pronounced because the foundation has a greater coarse particle content. The reinforcement effect diminishes with increasing distance from the vibrator.

Keywords: vibroflotation; coral sand foundation; particle size distribution; excess pore water pressure; cone penetration test

check for updates

Academic Editor: Decheng Wan

Received: 7 March 2025
Revised: 24 March 2025
Accepted: 25 March 2025
Published: 26 March 2025

Citation: Xin, Y.; Ding, X.; Zhao, J.; Wang, H.; Jiang, C. A Study on the Response of Coral Sand Foundations with Different Particle Gradations Reinforced Using a Vibroflotation Method. *J. Mar. Sci. Eng.* **2025**, *13*, 666. https://doi.org/10.3390/jmse13040666

Copyright: © 2025 by the authors. Licensee MDPI, Basel, Switzerland. This article is an open access article distributed under the terms and conditions of the Creative Commons Attribution (CC BY) license (https://creativecommons.org/licenses/by/4.0/).

1. Introduction

In recent years, land reclamation activities on islands have been rapidly expanding with the continuous development of marine engineering [1,2]. Many island facilities, such as airport runways, ports, and coastal defense projects, are typically constructed on coral sand foundations formed via hydraulic filling [3–5]. Coral sand foundation is a unique type of geotechnical material [6–8], which is primarily composed of calcium carbonate, characterized by high internal porosity [9,10], irregular particle shapes [11,12], and high permeability [13]. Numerous experimental studies have been conducted on coral sand from various perspectives, including its mechanical properties [14–16], particle breakage characteristics [17,18], bearing capacity [19,20], and liquefaction behavior [21–23].

The loose coral sand foundation formed by hydraulic filling is susceptible to hazards such as earthquake-induced liquefaction and uneven settlement [24]. It is necessary to adopt simple and efficient foundation treatment technology to strengthen the artificial islands formed by hydraulic filling [25]. Sand foundation is usually reinforced by impact rolling [26], which is only effective for the surface foundation, but the treatment effect of the deep foundation is poor [27]. Dynamic compaction compresses the foundation through the impact load exerted by heavy objects to increase the foundation strength [28,29], but the treatment effect is not obvious for the foundation below the groundwater level [30]. Vibroflotation is an effective method for treating sand foundations. It densifies loose sand through the horizontal vibration of a vibroflotation device [31], which has been effectively proven in the coral sand foundation treatment project [32,33]. Through field tests, Massarsch et al. [34] compared the increase in horizontal effective stress among five different foundation compaction methods. Wang et al. [33] applied vibroflotation to treat a dredged coral sand foundation and made improvements for the problem of weak silt and fine sand interlayers. Nagy et al. [35] analyzed the interaction between the vibrator and soil by monitoring the movement of the vibrator. Greenwood et al. [36] divided the soil around the vibrator into five zones, suggesting that only the transition and densification zones exhibit significant densification effects. Numerical simulation techniques have been used by researchers to compare factors such as the spacing between vibroflotation points [37], the vibration frequency [38], and the working depth of the vibrator [39]. Nagula et al. [38] found that the degree of foundation reinforcement increases with the frequency of the vibrator. Nagula et al. [40] studied the vibroflotation compaction process in fine sand foundations. Triantafyllidis et al. [41] estimated the strength and extent of the reinforced area using the high cycle accumulation model (HCA). In indoor model tests, Zhao et al. [42,43] compared the effect of the working parameters of the vibrator on the reinforcement effect of vibroflotation and tested the liquefaction resistance of the ground after vibroflotation through shaking-table tests. In summary, scholars have conducted extensive research on the vibroflotation method for foundation reinforcement through field tests, numerical simulations, and model tests, thereby laying a solid foundation for its theoretical development and engineering applications.

During the hydraulic filling process in island reclamation, coral sand particles initially settle under their own weight to establish the foundation; however, they are simultaneously influenced by water flow forces and hydraulic separation effects. This interplay of gravitational settling and hydrodynamic sorting leads to significant particle size segregation, ultimately resulting in a highly uneven and discontinuous particle size distribution across various locations within the dredged reclamation area.

During the hydraulic filling process, coral sand particles gradually settle under the influence of gravity. Due to differences in particle size and water flow, segregation occurs during the settling process, resulting in a discontinuous distribution of gradation in the foundation [24]. This uneven grain distribution, especially the degree of mixing between coarse and fine particles, directly affects the strength of the foundation [33]. Dong et al. [44] analyzed the particle size segregation behavior during the dredging process, and the grain distribution of the foundation formed by hydraulic filling is often discontinuous. Currently, there is relatively little research on the influence of particle size distribution on the reinforcement of coral sand foundations using vibroflotation. Through the indoor model test, the characteristics of foundation change can be accurately analyzed, and then the working parameters of the vibrator under different particle size distributions can be optimized.

This study utilizes a simulated vibrator system to conduct a series of laboratory experiments. The primary objectives are to investigate the response of coral sand foundations

reinforced by vibroflotation and to evaluate how the working parameters of the vibrator influence the behavior of the vibroflotation process. By analyzing the variations in EPWP and horizontal earth pressure during the vibroflotation process and employing the CPT to evaluate the effectiveness of foundation reinforcement. The research results can provide some valuable insights for the design of foundation treatment in coral sand sites.

2. Experimental Methods

2.1. Test Material and Facility

Three different gradations of coral sand were selected, with mass fractions of the 2–5 mm particle group being 53%, 23%, and 2%, respectively, representing the three types of foundations formed after particle segregation. The coral sand used in this study was sourced from an island in the South China Sea. The gradation curve of the coral sand is represented by the red line in Figure 1, and the physical parameters are detailed in Table 1.

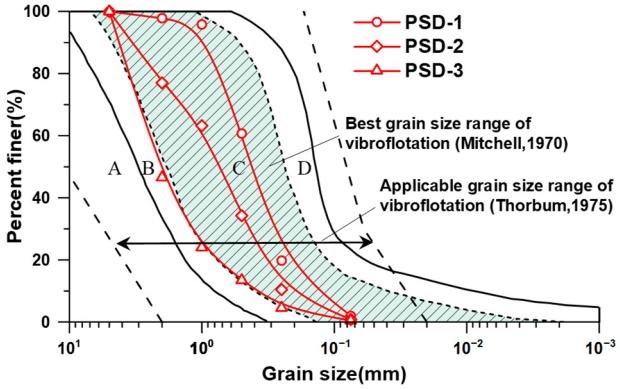


Figure 1. Particle size distributions of the coral sand [45,46].

Table 1. Physical properties of coral sand.

Particle Gradations	Effective Diameter, D_{10} (mm)	Coefficient of Uniformity, C_u	Specific Gravity, G_s	Maximum Dry Unit Weigh, $\gamma_{d.max}$ (kN/m^3)	Minimum Dry Unit Weigh, $\gamma_{d.min}$ (kN/m^3)
PSD-1	0.13	3.79	2.8	15.814	12.949
PSD-2	0.25	3.72	2.8	15.608	12.763
PSD-3	0.39	6.44	2.8	14.774	11.537

The effective particle size distribution range for a foundation reinforced by the vibroflotation has been proposed, as shown in Figure 1. Thorburn et al. [45] provided a broader range of soil particle gradation suitable for vibroflotation. Mitchell et al. [46] further proposed both the applicable and optimal gradation ranges for vibroflotation, as depicted in the shaded portion of Figure 1. Generally, the D region on the right side of the shaded area has too many fine particles, making it difficult to reinforce the foundation. When the gradation is entirely within the A region or partially within the B region, it significantly affects the penetration rate of the vibrator and the reinforcement effect. Conversely, when the curve is primarily distributed within the C region, it represents the optimal area for reinforcement using vibroflotation. The three different gradations are primarily situated within the optimal reinforcement range for the vibroflotation (within the shaded area).

The test model box measures 800 mm × 800 mm × 800 mm (with a soil fill height of 700 mm). The inner walls of the model box are lined with 0.5 cm thick EPE polyethylene foam for vibration isolation, reducing the reflection of vibration waves from the box walls.

The vibrator system, independently designed for indoor model tests, is depicted in Figure 2. The vibrator (1) has a diameter of 60 mm and a length of 600 mm. The frequency can be adjusted within the range of 0 to 50 Hz via the control cabinet (4). The vibrator is driven by a power motor connected via a flexible shaft, and its upward and downward penetration process is controlled by a chain block (3), resulting in effective reinforcement of the foundation. Additionally, a scale on the vibrator casing is employed to control the speed of the vibrator. While the guider (2) restricts its vertical movement, it also positions the vibro-compaction point (vibro-point) at the center of the model box by adjusting the position of the guider.

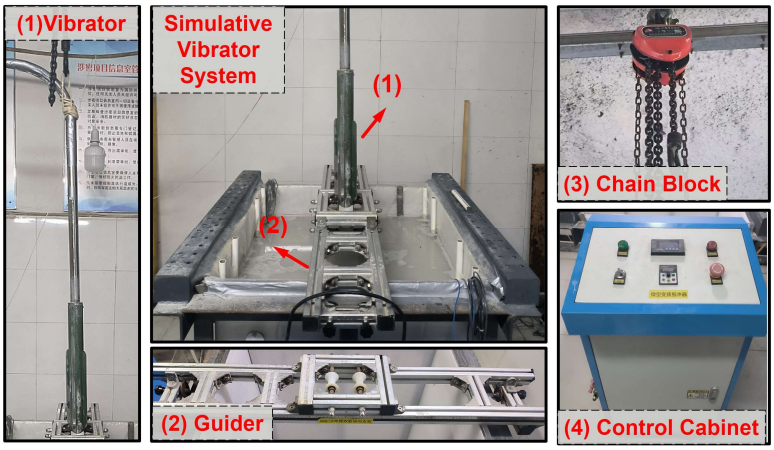


Figure 2. Sketches of testing equipment.

The upper section of the model box is fitted with a fixed support, which secures the driving motor by means of a detachable reaction frame. The driving motor propels the CPT cone downward at a consistent velocity. This arrangement enables the measurement of the cone tip resistance of the model foundation both prior to and after the test, and it can also be utilized to verify the uniformity of the foundation. To reduce the error caused by the boundary condition, a miniature CPT probe with a size of 5 cm^2 was selected for the experiment [47,48].

2.2. Model Preparation and Sensor Layout

To simulate the compaction degree of a real deposited foundation, the model foundation was prepared using the dry pluviation deposition method. Based on previous research, a relative density of 30% was chosen to simulate the loose state of the real dredged coral sand foundation. In the early stages of the experiment, parameters for the dry pluviation deposition method were calibrated for each gradation to ensure that the relative density of each model foundation was consistent. After the model foundation was prepared, water was slowly added to the pre-laid PVC pipes, allowing the water level to gradually seep upwards from the bottom of the foundation. The PVC pipes were perforated and wrapped with a fine mesh to prevent the coral sand from flowing into the pipes. The foundation was left for 24 h after water injection to ensure full saturation, which can effectively enhance the reinforcement effect of vibroflotation. During the foundation preparation process, the total mass of the coral sand was weighed to verify the initial relative density of the foundation. The saturated unit weight and effective unit weight of the foundation were calculated in the initial state, with relevant parameters detailed in Table 2.

Table 2. Parameters of initial model ground.

Particle Gradations	Dry Density ρ_d (g/cm^3)	Relative Density D_r/%	Saturated Unit Weight γ_{sat}/(kN/m^3)	Effective Unit Weight Γ'/(kN/m^3)
PSD-1	1.395	29.6	18.97	8.97
PSD-2	1.374	29.1	18.83	8.83
PSD-3	1.257	29.4	18.08	8.08

Figure 3a shows the sensor setup and position of CPT, and Figure 3b shows the specific layout of the sensor. A total of 12 earth pressure gauges and 12 pore pressure gauges were placed at designated locations during the model preparation process. The earth pressure gauges are designated as T, while the pore pressure gauges are marked as P. These instruments are utilized to record the changes in horizontal earth pressure and pore pressure responses of the model foundation during the vibroflotation reinforcement process. The positions of CPT testing are located at 0 mm, 200 mm, and 350 mm away from the vibro-point, which are used to determine the reinforcement influence range of single vibroflotation.

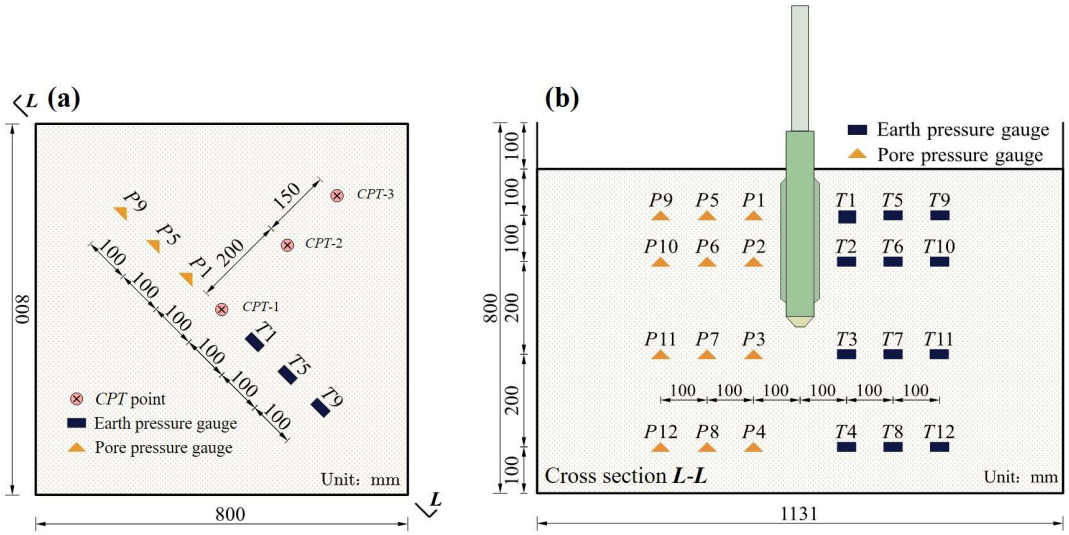


Figure 3. Sensor setup and position of CPT: (**a**) plane, (**b**) cross-section *L-L*.

It is important to note that the sensors were arranged along the diagonal of the box. Both types of sensors are symmetrically placed at both ends of the central vibro-point, with all earth pressure gauges oriented towards the direction of the vibro-point to record changes in horizontal earth pressure. Figure 3b shows that the pore pressure gauges P1-P12 and earth pressure gauges T1–T12 are arranged at distances of 100 mm, 200 mm, and 300 mm from the vibro-point, divided into near, medium, and far distances. They are also arranged in four layers at depths of 100 mm, 200 mm, 400 mm, and 600 mm from the surface of the model foundation.

2.3. Test Cases and Procedures

To explore the impact of gradation on the reinforcement of coral sand foundation using vibroflotation, a total of five test cases were designed, incorporating three research variables. The detailed information of the five cases is shown in Table 3. The vibration duration is defined as the total time of vibration from the moment the vibrator penetrates to the bottom of the foundation until it is lifted.

Table 3. Test cases of the vibroflotation methods.

Cases	Particle Gradation	Vibration Duration (s)	Vibration Frequency (Hz)	Times of Vibrations
1#	PSD-1	100	50	3
2#	PSD-2	100	50	
3#	PSD-3	100	50	
4#	PSD-2	50	50	
5#	PSD-2	100	25	

The complete steps of a test procedure are as follows: (1) Prepare the model foundation and saturate it for 24 h; (2) the CPT device was installed, and tests were conducted on the initial foundation at designated points. Afterward, the device was dismantled; (3) fix the guider at the center of the model box, and place the vibrator in it; (4) turn on the vibrator and penetrate it to the bottom at a uniform speed of 1 cm/s. Then, the vibrator works according to the vibration duration; (5) lift the vibrator at a uniform speed of 1 cm/s to the surface of the foundation; (6) after a brief interval, repeat steps 4 and 5 to conduct two additional vibrations; (7) after the vibration is complete, make the foundation rest for 24 h to facilitate drainage and consolidation; (8) repeat step 2 to detect changes in the foundation strength after vibroflotation; (9) data analysis.

It is important to note that for Case 5, the vibration frequency of only 25 Hz was insufficient to provide adequate penetration frequency, resulting in incomplete penetration to the bottom of the foundation during the second and third vibrations, with depths of only 45 cm and 35 cm, respectively. In contrast, the other cases successfully penetrated to the bottom of the foundation during the tests.

3. Results and Discussion

3.1. Compaction Phenomenon of Vibroflotation Reinforcement Foundation

Figure 4 shows the performance changes in the coral sand foundation during the vibroflotation reinforcement process. As shown in Figure 4a, the ground surface exhibited only partial water coverage before vibroflotation. However, as the vibrator began to penetrate downward, a significant amount of water gushed out from the ground surface. Concurrently, the foundation gradually compacted, and the ground surface progressively sank. During the vibroflotation process, fine particles within the foundation migrated upward around the vibrator, resulting in the turbidity of the upper water and the formation of foam [49], as shown in Figure 4b. At this stage, with the increase in vibroflotation times, the foundation settlement was obvious. After the vibroflotation, the water within the model cleared after 24 h of rest, and a vibrator pit formed at the vibro-point, as illustrated in Figure 4c. It is evident that there was significant uneven settlement on the surface of the foundation after the test, and a vibrator pit was formed at the vibro-point. The ground surface settlement was obviously related to the distance from the vibro-point after vibroflotation. There was a bulge in the center of the foundation, which was caused by the loosening and volume increase in the soil around the vibrator after the last vibroflotation ended, reducing the strength of the compacted shallow foundation.

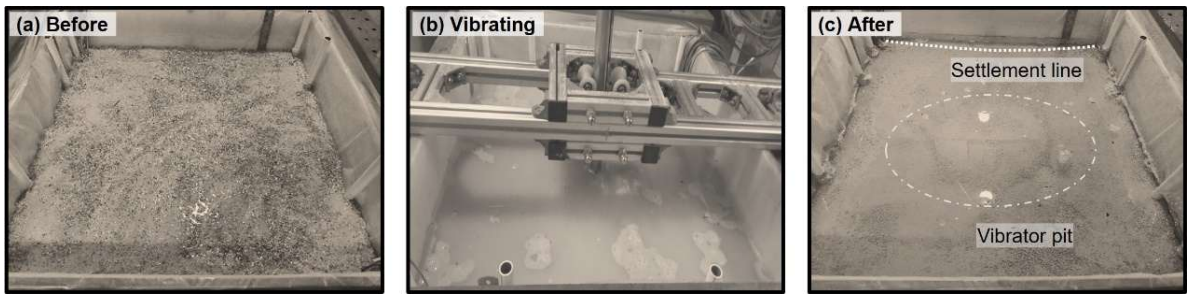


Figure 4. Performance of coral sand foundation in vibroflotation reinforcement process.

Table 4 presents the surface settlement around the vibro-point for Case 2 after each vibration. The settlement decreases radially outward from the vibro-point, creating a basin-like surface with the maximum settlement at the center of the vibro-point. The magnitude of the settlement is significantly correlated with the distance from the vibro-point. As the distance from the vibro-point decreased, the foundation settlement increased, and the reinforcement effect became more pronounced. After the first vibroflotation, the settlement was the most significant. The settlement during the second and third vibroflotation was significantly reduced compared to the first. Additionally, with each subsequent foundation reinforcement, the amount of foundation settlement decreased, indicating that the reinforcement effect of the foundation was most noticeable during the first vibroflotation. And the compaction effect gradually diminished with increasing vibroflotation.

Table 4. Surface settlement around the vibro-point.

Times	Distance from Vibro-Point (cm)		
	10	**30**	**50**
1	4.5	3.5	1.8
2	1.0	1.1	0.2
3	0.3	0.4	0.2
Resting for 24 h	0.2	0.2	0.1

3.2. Relative Density

Figure 5 shows the average relative density changes in the foundation around the vibro-point, which were calculated based on the cumulative surface settlement data presented in Table 4. As shown in Figure 5, the relative density increases with the times of vibration. After three vibration compaction treatments, the relative density at the vibro-point increased from 29.1% to 63.6%, 70.51%, and 72.5%, respectively, representing an increase of nearly 2.5 times. The intermediate results were estimated using cubic interpolation. With a relative density of 66% as the criterion, the radius of the area with a density greater than 66% after three vibrations was 32 cm, which is five times the diameter of the vibrator. Of course, the reinforcement effect is closely related to the power and frequency of the vibrator.

After three vibration reinforcements, the foundation transitioned from a loose to a dense state, with a significant increase in relative density following the first treatment. This is because the loose foundation formed by hydraulic filling has a high void ratio. The continuous vibration of the vibrator causes the particles to rearrange and densify during the vibro-compaction, effectively reducing the void ratio and increasing the relative density. The increase in relative density after the first vibroflotation was significantly greater than that after the subsequent two reinforcements. It is particularly observed that the foundation experienced minor settlement within 24 h of rest. This is because the EPWP had largely dissipated within one hour after vibroflotation [50]. This leads to a slight settlement of the

ground surface after reinforcement. However, the increase in soil strength is slower than the dissipation of EPWP. The improvement of soil strength after vibroflotation is closely related to the increase in effective stress caused by the dissipation of EPWP [51]. As the EPWP dissipates, the effective stress of the foundation increases, which enhances the soil strength.

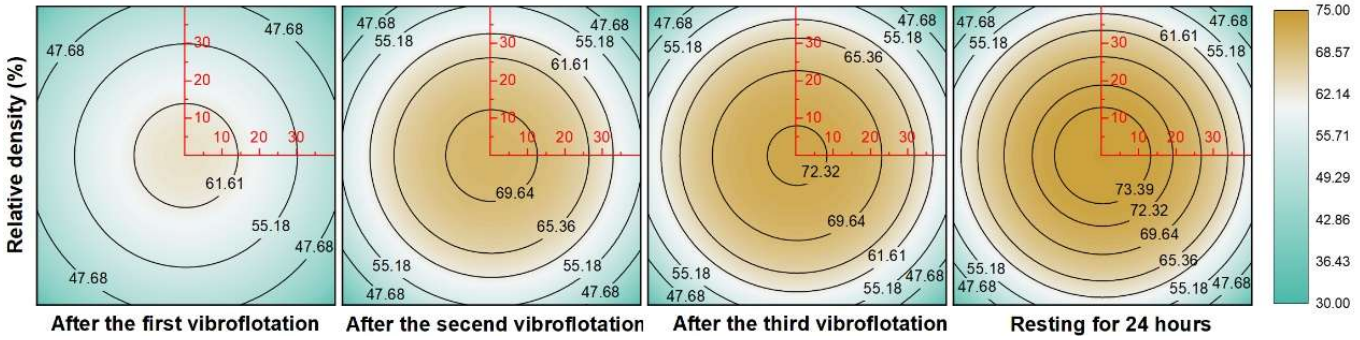


Figure 5. The variation in relative density with the times of vibroflotation.

As shown in Figure 5 and the peripheral settlement line in Figure 4c, the maximum settlement occurs at the center of the vibro-point, while the minimum settlement occurs on both sides. The influence range of the vibrator is centered on the vibro-point and radiates outwards through the vibration of the vibrator. The effectiveness of the vibroflotation decreases with increasing radius [36]. It is important to note that the vibration frequency of the vibrator significantly affects the reinforcement effectiveness of different graded foundations. During the vibroflotation process, it was observed that for the PSD-2 gradation, the reinforcement effect was significantly lower when using 25 Hz. There was no significant turbidity observed in the upper water. This is mainly due to the lower vibration frequency, which did not induce the foundation to liquefy. In Case 5, at 25 Hz, the vibrator did not fully penetrate during the second and third insertion processes, only reaching partial depth. The selection of the vibrator frequency is not only related to the compaction effect of the vibrator on the foundation but also to the penetration depth of the vibrator. Selecting a vibroflotation frequency that resonates with the soil can better transmit energy into the foundation. The resonance effect promotes the arrangement and compaction of particles, thereby improving the reinforcement effect [52]. However, a vibration frequency that is too high, while facilitating the penetration of the vibrator, does not contribute to the compaction of the foundation [50]. It is necessary to select an appropriate vibration frequency and power to effectively reinforce the foundation in practical engineering.

3.3. Time History of Excess Pore Pressures

Periodic vibrations and compaction are generated by the vibrator in the sand foundation, causing EPWP to be produced in the surrounding sand. Figure 6 shows the time history curves of EPWP for P1–P4 during the vibroflotation process of Case 2, reflecting the changes in EPWP response at different depths on one side of the vibrator. Based on the changes in EPWP during the vibroflotation process, the vibroflotation can be divided into three stages: the penetration stage, the vibration stage, and the lifting stage. In the penetration stage, the vibrator initiates its downward penetration, and the EPWP in the foundation exhibits a rapid increase to a peak value. This peak value escalates with increasing soil depth. In the vibration stage, the vibrator reaches the designated position and vibrates for a set duration. After reaching its peak, the EPWP gradually dissipates and eventually stabilizes at a constant value. During this stage, the foundation had already formed a compact structure under the squeezing action of the vibratory load. In the final lifting stage, the vibrator is progressively raised. Following the lifting vibrator, the EPWP

exhibits a brief fluctuation. When the vibrator is lifted, a cavity forms at the bottom of the vibrator, and the compacted soil loosens. Subsequently, the soil is dynamically filled under the action of the vibrator.

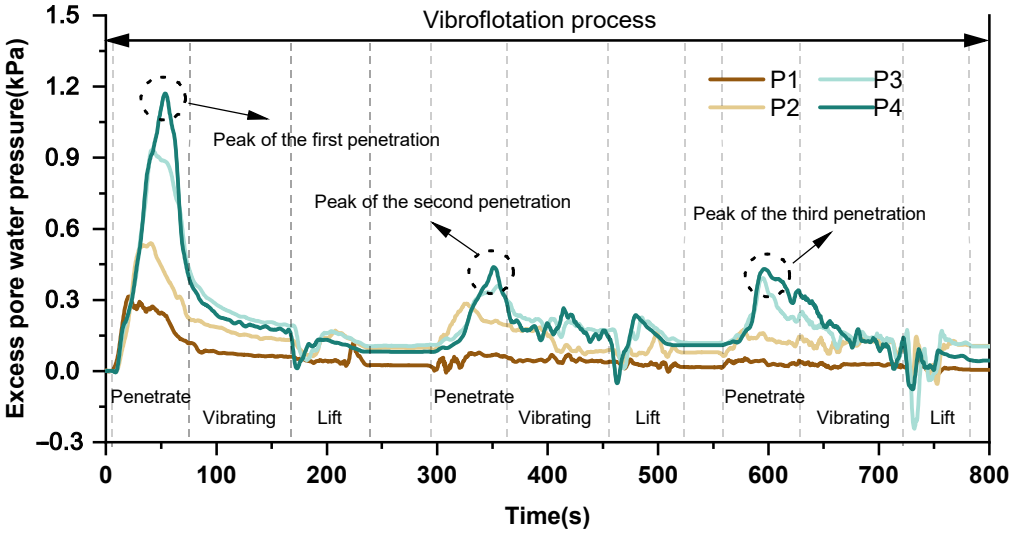


Figure 6. Time history curves of excess pore water pressure of Case 2.

During the three times of vibroflotation, the peak value of EPWP was greatest after the first penetration, and it decreases sequentially with subsequent vibroflotation. The reinforcement effect is notably significant after the first vibroflotation, but it gradually diminishes at the times of reinforcement. Research has indicated that an increase in the relative density of the foundation leads to a reduction in EPWP [53–55]. Observations of the gradual reduction in the peak of EPWP during multiple vibroflotation processes indicate a progressive increase in the relative density of the foundation.

It is noteworthy that the peak of pore water pressure recorded by sensor P1 is lower than that of the other sensors. Furthermore, during vibration, the EPWP stabilizes within a relatively narrow range. This is because the overburden pressure significantly influences EPWP. The overburden pressure increases in deeper regions. During the vibroflotation process, the overburden soil enhances the reinforcement effect of the vibrator. Due to the relatively low overburden pressure, the shallow foundation is easily disturbed during the vibration process, resulting in a lower (EPWP). The reinforcement effect of vibroflotation increases with depth, whereas its effect on shallow foundation is relatively limited. Therefore, it is essential to employ alternative methods, such as dynamic compaction, to further reinforce the shallow foundation at the surface [28,56,57].

3.4. Peak Excess Pressure and Excess Pore Pressure Ratio

The reinforcement of sand foundation by vibroflotaiton is that the pore water pressure increases instantaneously through the periodic vibration of the vibrator, resulting in temporary liquefaction of foundation. This process causes local sand particles to transition from a static state to a floating state, allowing the particles to rearrange during this process. Consequently, the densification of the foundation is enhanced after the dissipation of the pore water pressure. Assessing the degree of liquefaction is an effective way to determine the reinforcement effectiveness. The excess pore pressure ratio, r_u is an important indicator for evaluating the liquefaction of the sand foundation.

$$r_u = \frac{\Delta u}{\sigma'} \tag{1}$$

where Δu represents the excess pore water pressure at a certain depth, and σ' is the corresponding initial effective vertical stress.

Figure 7 shows the variations in EPWP and the corresponding excess pore pressure ratio for P1–P4 during the first penetration process. As shown in Figure 7a, the peak of EPWP during penetration increases with depth. It shows a significant effect of differences in particle gradation and vibroflotation techniques on the accumulation of pore pressure during vibroflotation. Because the content of initial gradation of coarse particles is higher, there is a more pronounced reduction in the peak of EPWP. The increased content of coarse particles leads to the formation of larger drainage channels between the particles, which promotes the rapid dissipation of pore water. This results in a longer accumulation process for EPWP, ultimately leading to different peaks of EPWP. From the perspective of energy conservation, a greater amount of energy is required to induce soil liquefaction as the content of coarse particles increases. When the energy of the vibrator is kept constant, the energy consumed by particle movement increases with particle size, while the energy used to work on water decreases. Consequently, there is a significant reduction in the peak of EPWP as the content of coarse particles increases.

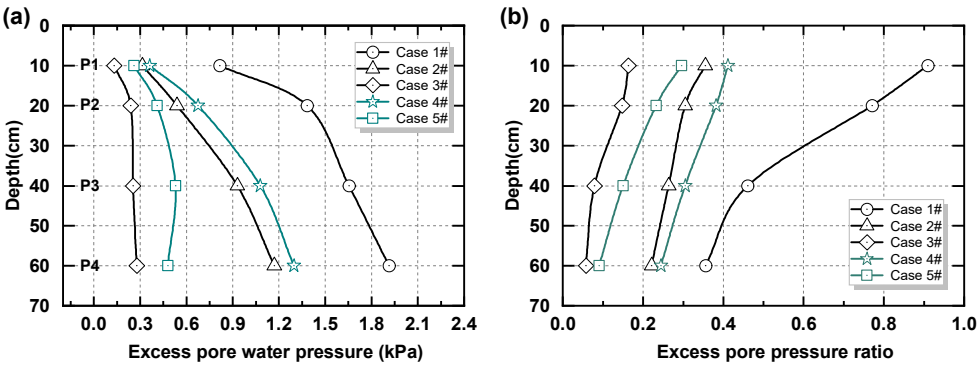


Figure 7. Comparison of the first penetration of vibro-point along depth: (**a**) excess pore water pressure; (**b**) excess pore pressure ratio.

Different work parameters of the vibrator also have a significant impact on the peak of EPWP. When the frequency of the vibrator was reduced from 50 Hz to 25 Hz, a noticeable decrease in peak pore pressure was observed, with the reduction becoming more pronounced at greater depths. The results of the excess pore pressure ratio corresponding to the peak pore pressure are shown in Figure 7b, which demonstrates that EPWP and the excess pore pressure ratio exhibit two distinct development trends. With the excess pore pressure ratio generally being significantly higher in the shallow layer compared to the deep layer. The excess pore pressure ratio of the foundation with a lower content of coarse particles is significantly higher than that of the foundation with a higher content. This is because the foundation with a higher content of coarse particles is less susceptible to liquefaction, resulting in a lower degree of liquefaction. Vibroflotation is employed to reinforce the foundation of a site with a higher content of coarse particles. The vibrator primarily densifies the foundation and reduces EPWP through horizontal vibration, thereby enhancing the bearing capacity of the foundation and its seismic resistance. To reinforce various foundations using vibroflotation, it is essential to select appropriate vibrator parameters to improve the reinforcement effect [43].

3.5. Earth Pressures in Horizontal Direction

To investigate the changes in particle compaction during the vibroflotation process, the horizontal earth pressure in the shallow and deep layers of the coral sand foundation was analyzed. This study selected the earth pressure time histories at the shallow location

(T6) and deep location (T8) from Case 1–3 for comparative analysis, as shown in Figure 8. Each earth pressure time history encompasses the penetration, vibration, and lift stages of the vibroflotation process. The vibrator applies horizontal cyclic loads to the soil through the rotation of an internal rotor, exerting a compressive force on the soil. Understanding the variations in earth pressure offers deeper insights into the foundation response during vibroflotation.

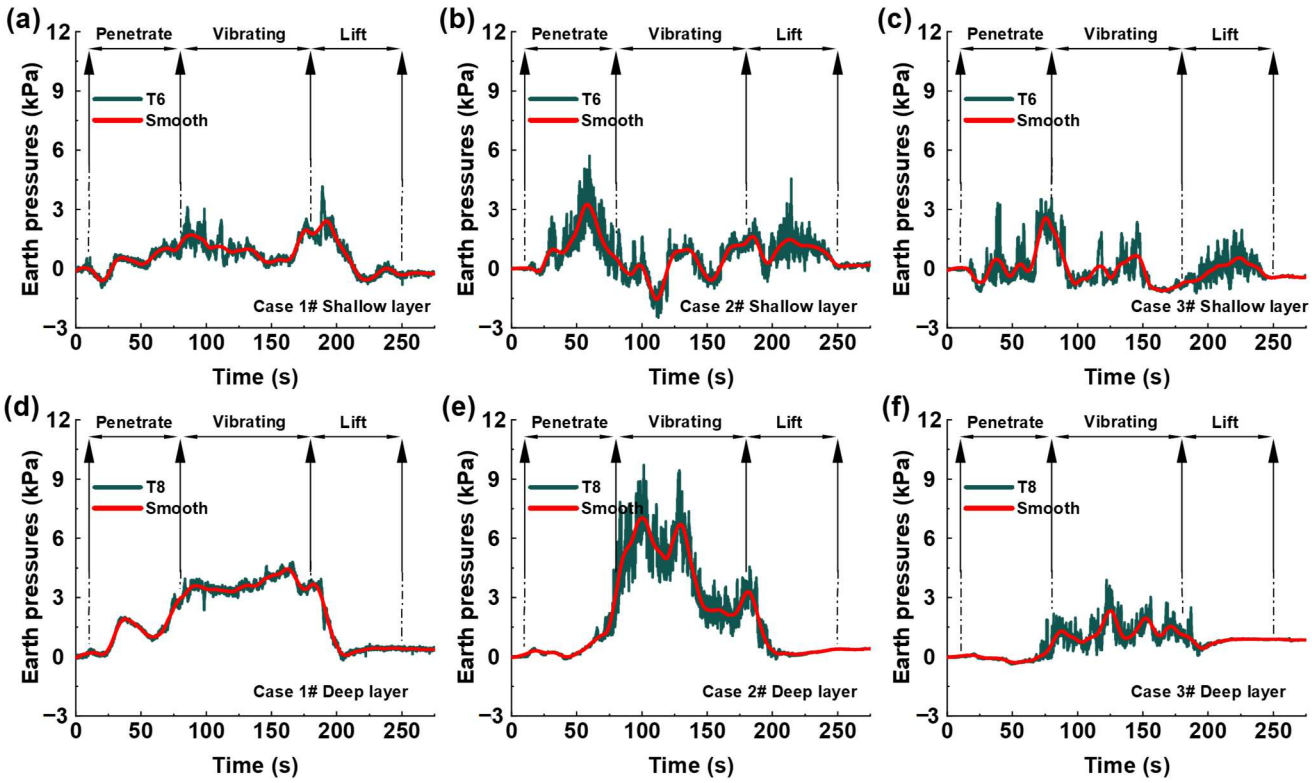


Figure 8. Time history curves of horizontal earth pressure in shallow and deep layers: (**a**) Case 1—T6, (**b**) Case 2—T6, (**c**) Case 3—T6, (**d**) Case 1—T8, (**e**) Case 2—T8, (**f**) Case 3—T8.

The results indicate a significant difference in the trend of earth pressure changes between the shallow and deep foundations. During the penetration stage, the earth pressure in the shallow foundation exhibits a characteristic of initially decreasing and then increasing. This is primarily due to the low initial relative density of the foundation. With the penetration of the vibrator, volume contraction of the soil particles occurred, leading to their downward migration. The effective stress within the foundation increases after the deep soil is reinforced through vibroflotation, and the surrounding soil is effectively compacted. Moreover, the degree of densification of the foundation increases with depth. However, the changes in earth pressure during the penetration stage were not significant in deep foundations.

Additionally, the earth pressure in the deep foundation remains at a high level during the vibration stage. It indicates that the reinforcement efficiency of the foundation reaches its maximum at this stage. During the lift stage, as the vibrator is gradually raised, cavities form at the bottom, resulting in sand backfilling into that area, which leads to a sudden decrease in horizontal earth pressure. During the vibration process, negative values of shallow earth pressure were observed. It is attributed to the downward movement of sand during the vibroflotation process, which leads to a reduction in effective stress.

The peak of shallow layer earth pressure occurred during the penetration and lift stages, whereas the peak of deep layer earth pressure was observed during the vibration stage. This indicates that particles exhibit two distinct modes of action at different depths

throughout the vibroflotation process. At the shallow layer, the upward and downward movements of the vibrator are likely to disturb the compacted soil, thereby weakening the reinforcement effect. At the deep foundations, the increased overburden pressure enables the vibrator to compress and compact the soil particles that have collapsed from the shallow layer. This results in the peak of deep earth pressure occurring during the vibration stage [41].

Due to the vibration-induced compaction, residual earth pressure exists in the horizontal earth pressure after the vibroflotation, indicating that the soil has been effectively reinforced, with increased contact stress between soil particles and a high degree of compaction. The changes in residual earth pressure after each vibroflotation can indicate the changes in particle compaction [34].

Figure 9 shows the changes in residual earth pressure after each vibroflotation. There is a significant difference between the residual horizontal earth pressure in the shallow layer (T6) and the deep layer (T8). The residual earth pressure of the deep layer is significantly higher than that of the shallow layer after each vibroflotation, and there is a clear trend of increasing earth pressure after each vibroflotation. This further indicates that the compaction degree of the foundation also rises with increasing times of vibroflotation reinforcement. It indicates that the deep layer is reinforced more effectively than shallow layer. After vibroflotation reinforcement, the foundation with three types of particle gradation reveals that the earth pressure in the deep layer significantly increases in Case 3. This demonstrates that a higher proportion of coarse particles in the foundation leads to better reinforcement effectiveness of the vibroflotation method.

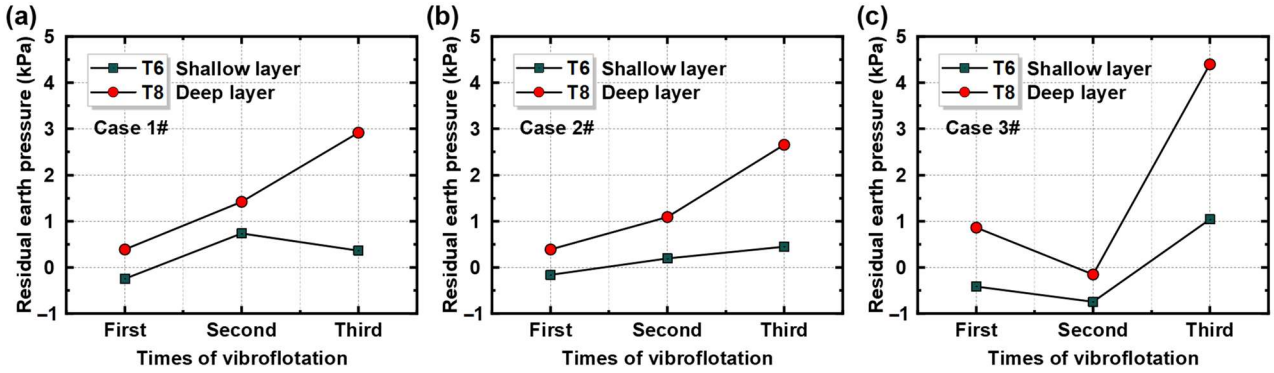


Figure 9. Variations in residual earth pressure after each vibroflotation: (**a**) Case 1, (**b**) Case 2, (**c**) Case 3.

3.6. Reinforcement Effectiveness Evaluation by CPT

Cone penetration tests were conducted before and after the vibroflotation to investigate the effectiveness and patterns of vibroflotation reinforcement. Figure 10 shows the cone tip resistance at different locations within the foundation before and after vibroflotation. From Figure 10a–c, it can be observed that the cone tip resistance exhibits a positive correlation with the distance from the vibro-point. Specifically, with closer distance to the vibro-point comes greater cone tip resistance, showing a more significant reinforcement effect on the foundation. The cone tip resistance at the vibro-point increases with a higher proportion of coarse particles in the foundation. This is attributed to the more pronounced rearrangement of particles during the vibroflotation process when the coarse particle content increases. Therefore, it improves densification and foundation strength significantly. In Case 3, the initial cone resistance is notably greater than that of the first two cases. This is primarily due to the angular characteristics of coral sand. After particle rearrangement during the vibroflotation process, the interlocking effect suppresses the relative particle rotation, thereby significantly increasing the shear strength of the foundation.

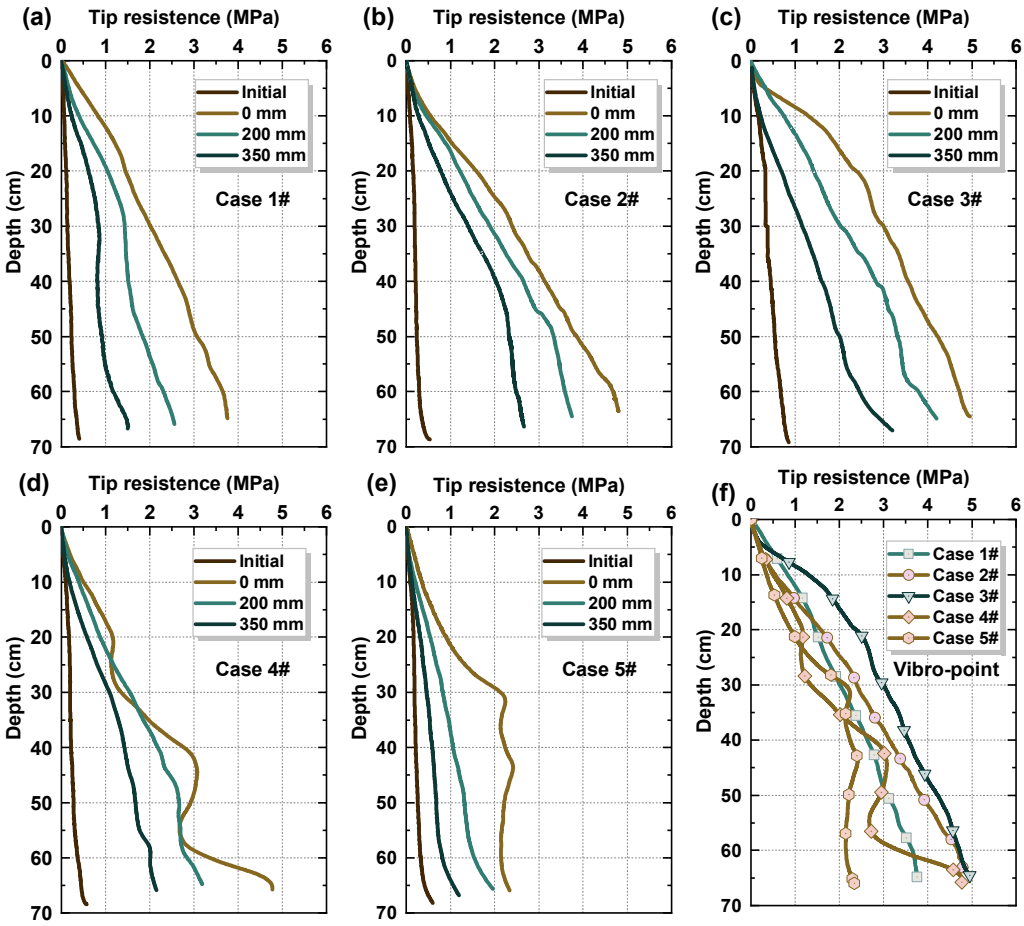


Figure 10. Tip resistance from CPT: (**a**) Case 1; (**b**) Case 2; (**c**) Case 3; (**d**) Case 4; (**e**) Case 5; (**f**) vibro-point.

From Figure 10a, it can be observed that the difference between the cone tip resistance at various locations after vibroflotation and the initial cone tip resistance of the foundation gradually increases as the depth increases. This indicates that the relative density of the foundation improves with increasing depth after vibroflotation reinforcement. In addition, the reinforcement effect is more significant at the deep layers, with the vibroflotation densification effect outperforming that at the shallow layers. Taking Case 1 as an example, the peak cone tip resistance values at various points after vibroflotation were compared to the initial foundation values. The cone tip resistance values at the vibro-point, as well as at distances of 200 mm and 300 mm from the vibro-point, increased by 9.4 times, 6.4 times, and 3.7 times, respectively. This indicates that there is a significant improvement in foundation strength, particularly within the area equivalent to six times the diameter of the vibrator.

From Figure 10d, it is evident that the cone tip resistance curve at the vibro-point does not exhibit the linear growth trend observed in Case 2 as depth increases. The average strength of the foundation is overall lower than that in Case 2. This phenomenon indicates that a reduced vibration duration results in insufficient effective energy output, thereby reducing the compaction degree of the foundation. Additionally, as shown in Figure 10e, the reduction in vibration frequency resulted in an insufficient effective vibroflotation frequency, causing the cone tip resistance to decrease by approximately twofold compared to Case 2. Under low-frequency working conditions, the vibrator failed to penetrate fully to the bottom of the foundation, further diminishing the reinforcement effect. This result indicates that the increasing vibration frequency not only significantly enhances the

reinforcement effect of the vibrator but also improves its penetration performance. Hence, the deep layers of the foundation can be adequately densified.

4. Conclusions

This study primarily investigates the influence of gradation on the foundation treatment of coral sand using vibroflotation through model tests. The changes in EPWP and horizontal earth pressure during the vibroflotation process were analyzed, and the effectiveness of foundation treatment was evaluated by CPT. The main conclusions are as follows:

(1) The maximum settlement of the coral sand foundation occurs after the first vibroflotation process. With the distance from the vibro-point decreasing, the settlement increases. As the times of vibroflotation increased, the reinforcement effect gradually diminished. The relative density of the foundation could be improved to a medium or dense state. Within 24 h after the completion of the vibroflotation, the foundation continued to experience slight settlement due to the dissipation of excess pore water pressure.

(2) During the penetration stage, the EPWP increases rapidly, significantly exceeding that of the vibration stage. As the times of vibration increase, the peak value of the EPWP gradually decreases, indicating improved soil compaction and reduced liquefaction potential. Shallow foundations demonstrate higher excess pore pressure ratios compared to deep foundations, exhibiting an inverse relationship with the distribution of peak EPWP.

(3) For coral sand foundations with fewer coarse particles, excess pore water pressure is significantly higher than in those with more coarse particles. Lower vibration frequency can reduce both the reinforcement effect and penetration depth in foundations with higher coarse particle content.

(4) The shallow layer peaks during the penetration and lift stage, while the deep layer peaks during the vibration stage. Foundations with higher coarse particle content exhibit greater residual soil pressure post-vibroflotation because of a more pronounced reinforcing effect in such foundations.

(5) After vibroflotation, cone tip resistance increases uniformly with depth and increases with distance from the vibro-point. Higher coarse particle content significantly enhances the relative density and the shear strength. Moreover, the vibration duration and frequency directly influence reinforcement effectiveness. It is necessary to select suitable vibro-compaction parameters for actual engineering.

Author Contributions: Methodology, X.D.; investigation, Y.X., X.D., J.Z., H.W. and C.J.; writing—original—draft, Y.X.; writing—review and editing, Y.X., X.D., J.Z., H.W. and C.J.; funding acquisition, X.D. All authors have read and agreed to the published version of the manuscript.

Funding: This work was supported by the Fundamental Research Funds for the Central Universities (No. 2022CDJQY-012).

Data Availability Statement: The original contributions presented in this study are included in the article. Further inquiries can be directed to the corresponding author.

Conflicts of Interest: Chunyong Jiang was employed by Chongqing City Construction Investment (Group). The remaining authors declare that the research was conducted in the absence of any commercial or financial relationships that could be construed as a potential conflict of interest.

References

1. Houlsby, G.T. Interactions in offshore foundation design. *Géotechnique* **2016**, *66*, 791–825. [CrossRef]
2. Sengupta, D.; Chen, R.; Meadows, M.E. Building beyond land: An overview of coastal land reclamation in 16 global megacities. *Appl. Geogr.* **2018**, *90*, 229–238. [CrossRef]
3. Song, N.Q.; Wang, N.; Lin, W.N. Assessment of the impact of artificial island airport reclamation on marine ecosystem health: A case study of the Dalian offshore airport, China. *Ocean Coast. Manag.* **2022**, *226*, 106281. [CrossRef]
4. Zhu, C.; Liu, H.; Wang, X.; Meng, Q.; Wang, R. Engineering geotechnical investigation for coral reef site of the cross-sea bridge between malé and airport island. *Ocean Eng.* **2017**, *146*, 298–310. [CrossRef]
5. Zhang, Y.; Ye, J.H. Physical modelling of the stability of a revetment breakwater built on reclaimed coral calcareous sand foundation in the south China sea—Random waves and dense foundation. *Ocean Eng.* **2021**, *219*, 108384. [CrossRef]
6. Qu, R.; Ma, C.H.; Zhu, C.Q.; Liu, H.F. Experimental study on the influence of particle morphology on compression characteristics of coral sand in south China sea. *Ocean Eng.* **2024**, *312*, 119339. [CrossRef]
7. Coop, M.R. The mechanics of uncemented carbonate sands. *Géotechnique* **1990**, *40*, 607–626. [CrossRef]
8. Giretti, D.; Fioravante, V.; Been, K.; Dickenson, S. Mechanical properties of a carbonate sand from a dredged hydraulic fill. *Géotechnique* **2018**, *68*, 410–420. [CrossRef]
9. Zhu, C.Q.; Chen, H.Y.; Meng, Q.S.; Wang, R. Microscopic characterization of intra-pore structures of calcareous sands. *Rock Soil Mech.* **2014**, *35*, 1831–1836. (In Chinese) [CrossRef]
10. Zhu, C.Q.; Zhou, B.; Liu, H.F. Investigation on strength and microstracture of naturally cemented calcareous soil. *Rock Soil Mech.* **2014**, *35*, 1655–1663. (In Chinese) [CrossRef]
11. Wang, X.; Wu, Y.; Cui, J.; Zhu, C.-Q.; Wang, X.-Z. Shape characteristics of coral sand from the south China sea. *J. Mar. Sci. Eng.* **2020**, *8*, 803. [CrossRef]
12. Wu, Y.; Cui, J.; Huang, J.; Zhang, W.; Yoshimoto, N.; Wen, L. Correlation of critical state strength properties with particle shape and surface fractal dimension of clinker ash. *Int. J. Geomech.* **2021**, *21*, 04021071. [CrossRef]
13. Jafarian, Y.; Javdanian, H.; Haddad, A. Strain-dependent dynamic properties of bushehr siliceous-carbonate sand: Experimental and comparative study. *Soil Dyn. Earthq. Eng.* **2018**, *107*, 339–349. [CrossRef]
14. Chen, Y.-Y.; Tang, Y.; Guan, Y.-F.; Liu, R.-M.; Han, X.; Zhao, X.-Q. Study on the mechanical properties of coral sands with different particle gradations. *Mar. Georesources Geotechnol.* **2023**, *41*, 327–338. [CrossRef]
15. Luo, Z.G.; Ding, X.M.; Ou, Q.; Zhang, T. Shear mechanical behavior of geogrid-reinforced calcareous sands under inclined reinforcement effects. *Int. J. Geomech.* **2025**, *25*, 04024355. [CrossRef]
16. Ke, L.; He, Y.; Chen, G.X. Experimental study of dynamic shear modulus and damping ratio characteristics of coral. *Rock Soil Mech.* **2020**, *41*, 23–31+38. [CrossRef]
17. Liu, F.; Tang, H.; Shahin, M.A.; Zhao, H.; Karrech, A.; Zhu, F.; Zhou, H. Multiscale simulation study for mechanical characteristics of coral sand influenced by particle breakage. *Powder Technol.* **2025**, *449*, 120387. [CrossRef]
18. Li, X.; Zhou, W.-H.; Liu, J.; Wang, C. Elastic-plastic response and particle breakage in marine coral sand: Roles of fines and density state. *Ocean Eng.* **2025**, *323*, 120499. [CrossRef]
19. Luo, Z.; Ding, X.; Zhang, X.; Ou, Q.; Yang, F.; Zhang, T.; Cao, G. Experimental and numerical investigation of the bearing capacity and deformation behavior of coral sand foundations under shallow footing loads. *Ocean Eng.* **2024**, *310*, 118601. [CrossRef]
20. Fang, X.; Shen, C.; Liu, H.; Wang, C.; Guo, Y.; Xiong, P.; Wang, L. Study on bearing characteristic of long-short-pile composite foundation with biocemented coral sand pile. *Acta Geotech.* **2025**, 1–11. [CrossRef]
21. Wu, Q.; Ding, X.M.; Zhang, Y.L. Joint analysis of macroscopic response and microfabric evolution of coral sand during earthquake-induced liquefaction. *Can. Geotech. J.* **2024**, *61*, 589–595. [CrossRef]
22. Sarajpoor, S.; Chen, Y.; Wang, Z.; Chen, R.; Ma, K. Experimental study on liquefaction behavior of desaturated calcareous sand under various stress conditions using air injection technique. *Soil Dyn. Earthq. Eng.* **2025**, *194*, 109363. [CrossRef]
23. Zhang, Z.X.; Chen, S.; Wang, Y.Z.; Li, X.J. Experimental study on the effect of an underground structure on the seismic responses of saturated coral sand site. *Appl. Ocean Res.* **2025**, *154*, 104392. [CrossRef]
24. Wang, X.; Ding, H.; Meng, Q.; Wei, H.; Wu, Y.; Zhang, Y. Engineering characteristics of coral reef and site assessment of hydraulic reclamation in the south China sea. *Constr. Build. Mater.* **2021**, *300*, 124263. [CrossRef]
25. Ding, X.M.; Luo, Z.G.; Ou, Q. Mechanical property and deformation behavior of geogrid reinforced calcareous sand. *Geotext. Geomembr.* **2022**, *50*, 618–631. [CrossRef]
26. Chen, Y.; Jaksa, M.B.; Kuo, Y.-L.; Airey, D.W. Experimental analysis of rolling dynamic compaction using transparent soils and particle image velocimetry. *Can. Geotech. J.* **2021**, *59*, 254–271. [CrossRef]
27. Virgil Ping, W.; Yang, Z.; Leonard, M.; Putcha, S. Laboratory simulation of field compaction characteristics on sandy soils. *Transp. Res. Rec.* **2002**, *1808*, 84–95. [CrossRef]
28. Feng, S.J.; Tan, K.; Shui, W.H.; Zhang, Y. Densification of desert sands by high energy dynamic compaction. *Eng. Geol.* **2013**, *157*, 48–54. [CrossRef]

29. Gu, L.; Yang, W.; Wang, Z.; Wang, J.; Ye, G. Response of a coral reef sand foundation densified through the dynamic compaction method. *J. Mar. Sci. Eng.* **2024**, *12*, 1479. [CrossRef]
30. Ke, J.; Ma, L.; Luo, Z.; Shi, X.; Song, Y.; Tan, Y. Compressibility and crushing of coral sands under one-dimensional dynamic compaction. *Granul. Matter* **2021**, *23*, 95. [CrossRef]
31. Slocombe, B.C.; Bell, A.L.; Baez, J.I. The densification of granular soils using vibro methods. *Géotechnique* **2000**, *50*, 715–725. [CrossRef]
32. Qiu, W.J.; Yang, H.P.; He, Y.X.; Yu, D.H. Experimental study on coral reef sand as hydraulic filling materials for foundation and its vibroflotation compaction. *Chin. J. Geotech. Eng.* **2017**, *39*, 1517–1523. (In Chinese) [CrossRef]
33. Wang, X.Z.; Ding, H.Z.; Wen, D.S.; Wang, X. Vibroflotation method to improve silt interlayers of dredged coral sand ground—A case study. *Bull. Eng. Geol. Environ.* **2022**, *81*, 472. [CrossRef]
34. Massarsch, K.R.; Wersäll, C.; Fellenius, B.H. Horizontal stress increase induced by deep vibratory compaction. *Proc. Inst. Civ. Eng.—Geotech. Eng.* **2020**, *173*, 228–253. [CrossRef]
35. Nagy, P.; Pistrol, J.; Kopf, F.; Adam, D. Integrated compaction control based on the motion behavior of a deep vibrator. *Transp. Geotech.* **2021**, *28*, 100539. [CrossRef]
36. Greenwood, D.A.; Kirsch, K. Specialist ground treatment by vibratory and dynamic methods. In *Piling and Ground Treatment*; The Institution of Civil Engineers: London, UK, 1984; pp. 17–45.
37. López-Querol, S.; Peco, J.; Arias-Trujillo, J. Numerical modeling on vibroflotation soil improvement techniques using a densification constitutive law. *Soil Dyn. Earthq. Eng.* **2014**, *65*, 1–10. [CrossRef]
38. Nagula, S.S.; Grabe, J. Coupled eulerian lagrangian based numerical modelling of vibro-compaction with model vibrator. *Comput. Geotech.* **2020**, *123*, 103545. [CrossRef]
39. Arnold, M.; Herle, I. Comparison of vibrocompaction methods by numerical simulations. *Int. J. Numer. Anal. Methods Geomech.* **2009**, *33*, 1823–1838. [CrossRef]
40. Nagula, S.; Nguyen, M.; Grabe, J.; Kardel, J.; Bahl, T. Field measurements and numerical analysis of vibroflotation of sand. *Géotechnique* **2022**, *72*, 882–898. [CrossRef]
41. Triantafyllidis, T.; Kimmig, I. A simplified model for vibro compaction of granular soils. *Soil Dyn. Earthq. Eng.* **2019**, *122*, 261–273. [CrossRef]
42. Zhao, J.; Ou, Q.; Chen, R.; Ding, X.; Wang, H. Seismic response of vibroflotation reinforced coral sand foundation through shaking table tests. *Appl. Ocean Res.* **2023**, *140*, 103738. [CrossRef]
43. Zhao, J.Q.; Ou, Q.; Ding, X.M.; Chen, Z.X. Model test study on the response of coral sand foundation reinforced by vibroflotation. *Acta Geotech.* **2023**, *18*, 6201–6212. [CrossRef]
44. Dong, Y.; Liu, C.; Wei, H.; Meng, Q.; Zhou, H. Size segregation mechanism of reclamation fill sand due to rainbowing operations in hydraulic dredging activities. *Ocean Eng.* **2021**, *242*, 109957. [CrossRef]
45. Thorburn, S. Building structures supported by stabilized ground. *Géotechnique* **1975**, *25*, 83–94. [CrossRef]
46. Mitchell, J.K. In-place treatment of foundation soils. *J. Soil Mech. Found. Div.* **1970**, *96*, 73–110. [CrossRef]
47. Sadrekarimi, A. Evaluation of cpt-based characterization methods for loose to medium-dense sands. *Soils Found.* **2016**, *56*, 460–472. [CrossRef]
48. Shirani, S.S.; Eslami, A.; Ebrahimipour, A.; Karakouzian, M. Dominant factors in minicone, cpt and pile correlations: A data-based approach. *Deep Undergr. Sci. Eng.* **2023**, *2*, 346–358. [CrossRef]
49. Zhao, J.Q.; Ding, X.M.; Liu, H.L.; Ou, Q.; Jiang, C.Y. Laboratory experiment study on response of vibroflotation compaction of coral sand. *Rock Soil Mech.* **2023**, *44*, 2327–2336+2349. (In Chinese) [CrossRef]
50. Zhou, J.; Wang, G.Y.; Cai, J.M. Situation and latest technical progress of vibroflotation without additional backfill treatment. *Rock Soil Mech.* **2008**, *29*, 37–42. (In Chinese) [CrossRef]
51. Zhou, J.; Jia, M.C.; Chi, Y. Vibroflotation compaction of silty fine sands without additional backfill materials. *Chin. J. Rock Mech. Eng.* **2003**, *22*, 1350–1355. (In Chinese) [CrossRef]
52. Rainer Massarsch, K.; Fellenius, B.H. Chapter 19 deep vibratory compaction of granular soils. In *Elsevier Geo-Engineering Book Series*; Elsevier: Amsterdam, The Netherlands, 2005; Volume 3, pp. 539–561.
53. Ecemis, N.; Demirci, H.E.; Karaman, M. Influence of consolidation properties on the cyclic re-liquefaction potential of sands. *Bull. Earthq. Eng.* **2015**, *13*, 1655–1673. [CrossRef]
54. Teparaksa, J.; Koseki, J. Effect of past history on liquefaction resistance of level ground in shaking table test. *Géotech. Lett.* **2018**, *8*, 256–261. [CrossRef]
55. Krim, A.; Arab, A.; Bouferra, R.; Sadek, M.; Shahrour, I. Characteristics of cyclic shear behavior of sandy soils: A laboratory study. *Arab. J. Sci. Eng.* **2016**, *41*, 3995–4005. [CrossRef]

56. Li, P.; Sun, J.; Ge, X.; Zhang, M.; Wang, J. Parameters of dynamic compaction based on model test. *Soil Dyn. Earthq. Eng.* **2023**, *168*, 107853. [CrossRef]
57. Chow, Y.K.; Yong, D.M.; Yong, K.Y.; Lee, S.L. Dynamic compaction analysis. *J. Geotech. Eng.* **1992**, *118*, 1141–1157. [CrossRef]

Disclaimer/Publisher's Note: The statements, opinions and data contained in all publications are solely those of the individual author(s) and contributor(s) and not of MDPI and/or the editor(s). MDPI and/or the editor(s) disclaim responsibility for any injury to people or property resulting from any ideas, methods, instructions or products referred to in the content.